

Adsorption Geometry Dependent Selective Bond Activation of Cyclic CH₂N₂ on Pd(110)

P. H. Mc Breen,* S. Serghini Monim, and M. Ayyoob

Contribution from the Département de chimie, Université Laval, Québec G1K 7P4, Canada.
Received August 2, 1991

Abstract: The adsorption of diazirine, cyclic CH₂N₂, on Pd(110) was studied using X-ray photoelectron spectroscopy and temperature-programmed desorption. Three chemisorbed states of diazirine are populated on Pd(110) at 107 K. The first state to grow in is characterized by a narrow N_(1s) feature at 398.3 eV, the second by a broad feature at 399.5 eV, and the third by a broad feature at 402.1 eV. We label the three adsorption states as the α -, β -, and γ -states, respectively. Angle-resolved XPS measurements and the observed N_(1s) peak width show that the latter feature arises from a highly tilted species with two inequivalent nitrogens. On the basis of the angle-resolved measurements, the binding energies, and the peak widths and with reference to the geometry of diazirine-metal complexes it is argued that the α - and β -states involve substantial π -bonding to the surface whereas the γ -state is bonded to the surface via a σ -donor bond. In the case of the γ -state, the NN bond of diazirine is tilted away from the surface, whereas for the α - and β -states the NN bond is roughly parallel to the surface. TPD measurements show that in addition to a molecular desorption state of diazirine, methane, ethylene, nitrogen, hydrogen cyanide, and hydrogen are evolved from the surface. Ethylene desorption is only observed for high initial surface coverages of diazirine. These results indicate that both CN and NN bond scission occur. Adsorbed methylene resulting from CN bond scission is characterized by a C_(1s) binding energy of 283.6 eV. NN bond cleavage results in the deposition of atomic nitrogen, which yields an N_(1s) feature at 396.9 eV, and a species which we assign to NCH₂ads as characterized by a C_(1s) peak at 285.5 eV and an N_(1s) peak at 398.3 eV. The formation of adsorbed CH₂ species is observed at 130 K and coincides with the removal of the γ -state. The cleavage of the NN bond occurs above 150 K and coincides with the attenuation of the α - and β -states. Therefore, we conclude that the adsorption geometry of diazirine on Pd(110) determines the selective activation of the NN and CN bonds. This behavior may be rationalized in terms of the frontier orbitals of diazirine and the different modes of chemisorption to the palladium surface. A σ -donor bond between diazirine and palladium results in the removal of electron density from an orbital that is bonding in CN and antibonding in NN. In contrast, π -back-donation between diazirine and palladium involves electron transfer to an orbital that is antibonding in NN. The surface chemistry of diazirine is then very dependent on the adsorption geometry given the fact that it is a strained molecule which contains latent molecular nitrogen and which may be activated at either the CN or the NN bond. The strong intramolecular driving force toward the elimination of molecular nitrogen is at the origin of the fact that the third adsorption state of diazirine on Pd(110) is the first to decompose on heating and that a fraction of the adsorbed molecule decomposes to eject free methylene into the gas phase. The metal surface serves to activate the various observed processes.

Introduction

Adsorption of simple molecules on metal surfaces typically displays a chemistry which involves the sequential filling of adsorption sites characterized by distinct adsorption energies and by distinct reactivities. For example, Poalta and Thiel¹ observed that the initial adsorption of benzene on Ru(110) is dissociative. Further exposure to benzene leads to a molecularly adsorbed state which desorbs between 120 and 180 K, and multilayer formation occurs at still higher exposures. The same type of behavior can be observed by direct spectroscopic techniques. An example is the adsorption of CO on Mo(110) for which Chen et al.² report that low coverages are characterized by a $\nu(\text{CO})$ stretching frequency of 1345 cm⁻¹ whereas higher exposures lead to the detection of a species characterized by a $\nu(\text{CO})$ value of 1935 cm⁻¹. The thermal decomposition of an adsorbed simple molecule such as ethylene³ involves the abstraction of hydrogen atoms from the adsorbed molecule by the surface and the formation of a metal-hydrogen chemisorption bond. The adsorbed hydrogen atoms may then, under suitable conditions, recombine to desorb as molecular hydrogen. The remaining hydrocarbon fragment usually undergoes further decomposition on the surface. However, more complex molecules may display a somewhat less typical behavior. For example, Liu and Friend⁴ report that the strained molecule 2,5-dihydrothiophene undergoes a reaction on Mo(110) wherein the sulfur atom is deposited on the surface and the remainder of the molecule reorganizes intramolecularly to achieve the elimination of gaseous butadiene. In this paper we present results for

the chemistry of diazirine on Pd(110). Despite its beautifully simple C_{2v} geometry, diazirine is a complex adsorbate from the following points of view. This cyclic isomer of diazomethane displays a strain energy of approximately 20 kcal mol⁻¹.^{5,6} Through decomposition it can generate molecular nitrogen, a species characterized by a very high bond energy. The NN bond in diazirine is, however, relatively weak. Fukui et al.,⁷ in a molecular orbital study of nitrogen fixation, used diazirine as a model for molecular nitrogen side-on bonded to a metal complex. The highest occupied molecular orbital of diazirine is nontypical.⁸ The HOMO orbital is derived from the symmetry-allowed mixing of the carbon 2p_y orbital with the out-of-phase combination of the two nitrogen lone pair orbitals. The resultant molecular orbital is predominantly CN bonding with some NN antibonding character. On the other hand, the LUMO orbital is a π^* orbital, as in the case of the prototypical adsorbate, CO. For diazirine, the latter orbital is essentially NN antibonding and is predicted to be situated at approximately -7.5 eV.⁸ The HOMO orbital of diazirine is located at approximately -11.5 eV.⁸ The predicted (EHT) values for the LUMO and HOMO orbitals of CO are -12.4 and -8.3 eV, respectively.⁹ Inverse photoemission studies typically place the electron affinity level of adsorbed CO at a few electronvolts above E_F, and UPS measurements on adsorbed CO

(1) Poalta, J. A.; Thiel, P. A. *J. Am. Chem. Soc.* **1986**, *108*, 7560.
(2) Chen, J. G.; Colaianni, M. L.; Weinberg, W. H.; Yates, J. T., Jr. *Chem. Phys. Lett.* **1991**, *177*, 113.
(3) Hills, M. M.; Parmenter, J. E.; Mullins, C. B.; Weinberg, W. H. *J. Am. Chem. Soc.* **1986**, *108*, 3554.
(4) Liu, A. C.; Friend, C. M. *J. Am. Chem. Soc.* **1991**, *113*, 820.

(5) Paulett, G. S.; Ettinger, R. J. *Chem. Phys.* **1963**, *39*, 825.
(6) Bigot, B.; Poncet, R.; Sevin, A.; Devaquet, A. *J. Am. Chem. Soc.* **1978**, *100*, 6575.
(7) Yamabe, T.; Hori, K.; Minato, T.; Fukui, K. *Inorg. Chem.* **1980**, *19*, 2154.
(8) Baird, N. C. In *Chemistry of Diazirines*; Liu, M. T. H., Ed.; CRC Press, Inc.: Boca Raton, FL, 1987; Vol. 1, Chapter 1.
(9) Lindholm, E.; Li, J. J. *J. Phys. Chem.* **1988**, *92*, 1731.
(10) Avouris, Ph.; DiNardo, N. J.; Demuth, J. E. *J. Chem. Phys.* **1984**, *80*, 491.

place the 5σ level at 8.5 eV below E_F .¹⁰ We assume that the electron affinity level of diazirine on palladium is also centered a few electronvolts above the Fermi level. Therefore, one might anticipate a similar donor-acceptor mode of bonding between diazirine and a transition-metal surface to that observed for chemisorbed CO. However, in the case of diazirine, the balance of donation and back-donation is critical in its consequences in that the molecule presents two different bonds, the CN bond and the NN bond, which may be activated. The chemistry of diazirine on Pd(110) does indeed display some unusual aspects. The results presented in this paper show that the third chemisorption state which is observed to populate on increasing the diazirine exposure is the first to dissociate on increasing the temperature. Furthermore, both CN and NN bond breaking is observed—a phenomenon which may be interpreted in terms of adsorption geometry dependent selective bond activation. An additional interesting aspect of diazirine chemistry on Pd(110) is that a fraction of the adsorbed species decomposes to yield gas-phase methylene.

In this paper we examine XPS and TPD data for the low-temperature range over which molecular diazirine is present on the surface. We use the results to characterize molecularly adsorbed states of diazirine and to correlate selective bond activation with the approximate adsorption geometry characteristic of each state. As a point of departure it is useful to briefly review results for the interaction of diazirines with organometallic complexes. Excellent reviews on this subject have been published by Kisch et al.^{11,12} Diazirines, cyclic isomers of R_2CN_2 , undergo ligand displacement reactions with Cr and W carbonyls forming one or two σ -bonds via the HOMO orbital. In addition to the above type of behavior, NN bond cleavage is observed for the interaction of diazirines with Fe and Ru carbonyls resulting in the formation of μ_2 -NCR₂ ligands. Recent work by Chaloner et al. shows that diazirines may be used for the synthesis of W, Cr, Rh, and Co carbene complexes.^{13–15} The Rh carbene complex is formed through the capture of free carbene resulting from thermolysis of the diazirine reagent. Carbene-generating molecules, such as diazirine, ketene, or diazomethane, play an important role in preparative organometallic chemistry and in the elucidation of reaction mechanisms in heterogeneous catalysis.¹⁶ They are thus excellent candidates for surface studies.^{17a–c} We find that diazirine displays a rich thermal and photon induced chemistry on Pd(110), and these results will be published separately.^{17e}

Experimental Section

The measurements were performed in an ion-pumped chamber. Typical base pressures were in the 10^{-11} -Torr range. The Pd(110) sample was mounted on a cold finger centered on a differentially pumped rotary platform. The details of the sample holder/cold finger and the manner in which the sample was mounted are similar to those described by Anderegg and Thiel.¹⁸ Resistive heating was used to provide a linear temperature ramp for the desorption measurements. The Pd(110) sample was cleaned by prolonged cycles of Ar ion bombardment and electron beam flashing to 1200 K. The remaining carbon was removed from the surface through exposure to O₂ and flashing to 1250 K. The hemispherical photoelectron spectrometer was mounted on the system with both the extended lens and the Al/Mg photon source oriented in the plane normal to the surface. Angle-resolved measurements were made by rotating the rotary platform. This arrangement also permitted line-

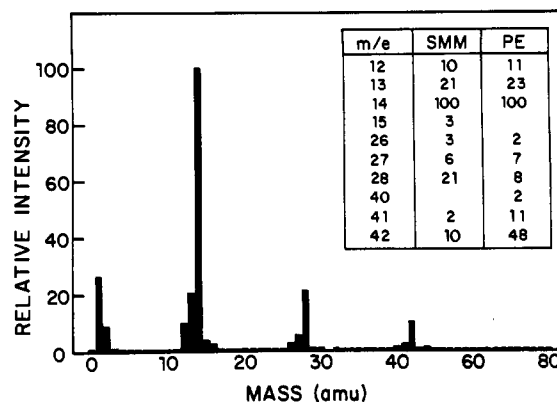


Figure 1. Mass spectrum of diazirine as measured on introduction into the UHV chamber. The relative abundances given in the inset refer to those measured by us (SMM) and those measured by Paulett and Ettinger (PE).²³

of-sight dosing of the sample, via stainless steel tubes, and line-of-sight desorption experiments. The quadrupole mass spectrometer was mounted in an enclosure and oriented at a polar angle of 45° to the surface normal. The QMS was interfaced to a PC compatible in order to operate in the multiplex mode, and five masses were followed during each desorption experiment.

Diazirine is a strained molecule.¹⁹ Although it is chemically inert it is thermally unstable. The same precautions as apply to diazomethane should be taken when working with diazirine. Diazirine may be stored over long periods at room temperature. However, the solid-liquid or the liquid-solid phase transition often leads to explosions. Considering the toxic nature of diazirine and the possibility of it exploding we chose to prepare a very small quantity of diazirine prior to each day's experiment. The total quantity prepared was always less than the TLV standard²⁰ for continuous exposure over 8 h. The synthesis was performed in situ under vacuum in a liquid N₂ trapped, turbomolecularly pumped, gas handling line. The gas handling line, which was attached directly to a leak valve on the UHV system, was constructed from stainless steel tubing, quickfit and miniflange connections, and kovar-Pyrex tube traps. The Pyrex tubes were coated on the outside with colloidal graphite in order to avoid photodecomposition effects. The entire gas handling system was enclosed in plexiglass with the toggles of the valves separating the traps protruding through. Similarly, the coolant dewars could be moved in and out of place using jacks thereby avoiding any line-of-sight exposure on the part of the operator. The entire plexiglass enclosure was pumped on by a ventilator.

Diazirine was synthesized following the procedure given by Ohme and Schmitz.²¹ In the first step of the synthesis a stock of methylenediamine sulfate was formed through the interaction of sulfuric acid with methylene diformamide obtained from the reaction of formamide with para-formaldehyde. Prior to each day's series of experiments, 0.3 g of the starting salt, methylenediamine sulfate, was placed in the first of the series of traps in the gas handling line. The system was then pumped down to less than 10^{-4} Torr, and an ice-water bath was placed around the first trap. The in situ reaction, to prepare diazirine, was initiated by adding, dropwise, 20 mL of sodium hypobromite to the salt. The oxidant was injected into the system, using a glass syringe, through a septum held vacuum tight by a CAJON Ultra-Torr fitting. The diazirine evolved was pumped through two traps at ~160 K (liquid N₂-cyclohexane slush) and into a liquid nitrogen trap where it was isolated and pumped on. Then, through the use of the toggle valves, a new pumping route was opened up and the diazirine was allowed to pass through another 160 K trap to reach a liquid N₂ trap located close to the leak valve where it could be sealed off. The diazirine was then transferred to and maintained in a trap at 160 K for the course of the experiment. The purity of the diazirine was verified using the quadrupole mass spectrometer. The mass spectrum is shown in Figure 1. The agreement with published spectra^{5,22} is excellent at $m/e \leq 28$. However, the relative intensity of the parent peak is lower by a factor of approximately 4.0 in our spectra. Calibration measurements with Ar were performed in order to rule out the possibility that this discrepancy was due to the mass spectrometer. We assume, based on the excellent agreement of the spectra at $amu \leq 28$, that we are

(11) Kisch, H. In *Chemistry of Diazirines*; Liu, M. T. H., Ed.; CRC Press, Inc.: Boca Raton, FL, 1987; Vol. II, Chapter 10.

(12) Albini, A.; Kisch, H. *Top. Curr. Chem.* **1976**, *65*, 105.

(13) Chaloner, P. A.; Glick, G. D.; Moss, R. A. *J. Chem. Soc., Chem. Commun.* **1983**, 880.

(14) Avent, A. G.; Benyunes, S. A.; Chaloner, P. A.; Hitchcock, P. B. *J. Chem. Soc., Chem. Commun.* **1987**, 1285.

(15) Benyunes, S. A.; Chaloner, P. A. *Organomet. J. Chem.* **1988**, *341*, C50.

(16) Brady, R. C.; Pettit, R. J. *J. Am. Chem. Soc.* **1981**, *103*, 1287, 1981.

(17) (a) George, P. M.; Avery, N. R.; Weinberg, W. H.; Tebbe, F. N. *J. Am. Chem. Soc.* **1983**, *105*, 1393. (b) Mc Breen, P. H.; Erley, W.; Ibach, H. *Surf. Sci.* **1984**, *148*, 292. (c) Radloff, P. L.; Mitchell, G. E.; Greenlief, C. M.; White, J. M.; Mims, C. A. *Surf. Sci.* **1987**, *183*, 377. (d) Serghini Monim, S.; Venus, D.; Roy, D.; Mc Breen, P. H. *J. Am. Chem. Soc.* **1989**, *111*, 4106. (e) Serghini Monim, S.; Mc Breen, P. H. In preparation.

(18) Thiel, P. A.; Anderegg, J. W. *Rev. Sci. Instrum.* **1984**, *55*, 1669.

(19) Schmitz, E., ref 9, Vol. 1, Chapter 3.

(20) TLV: air, 0.4 mg m⁻³. Sax, N. Irving *Dangerous Properties of Industrial Materials*, 6th ed.; Van Nostrand-Reinhold: Princeton, NJ.

(21) Schmitz, E.; Ohme, R. *Chem. Ber.* **1961**, *94*, 2166.

(22) Graham, W. H. *J. Am. Chem. Soc.* **1962**, *84*, 1063.

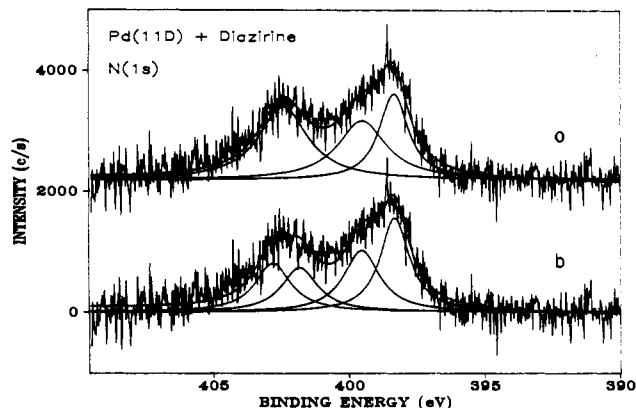


Figure 2. XPS spectrum in the $N_{(1s)}$ region for diazirine adsorbed on Pd(110) at 107 K. A three-peak fit to the spectrum is shown in a. In b, the broad high binding energy peak is resolved into two peaks.

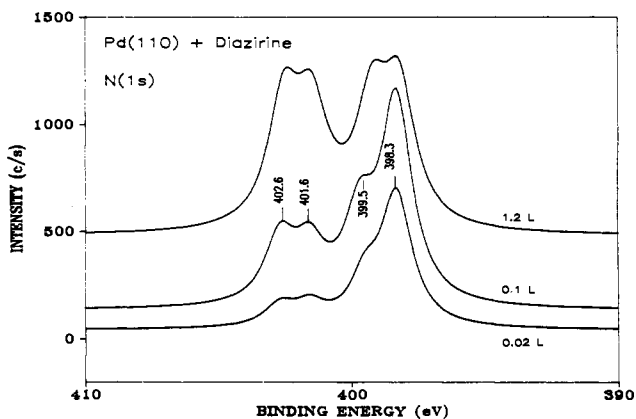


Figure 3. $N_{(1s)}$ spectra for diazirine adsorbed on Pd(110) at low ($\sigma_N = 4.2 \times 10^{14}$ atoms cm^{-2}), intermediate ($\sigma_N = 8.7 \times 10^{14}$ atoms cm^{-2}), and high ($\sigma_N = 1.46 \times 10^{15}$ atoms cm^{-2}) coverage. Surface concentrations, σ_N , were calculated following the procedure given by Carley and Roberts.⁵¹

preparing pure diazirine. The most likely contaminants in the case of diazirine are N_2 , ethylene, HCN, or azine resulting from the decomposition of diazirine. Decomposition of diazirine would also lead to methane formation through the interaction of the CH_2 diradical with the chamber walls. However, by comparison to the results of Paulett and Ettinger,⁵ the negligible intensity at m/e 27, 26, and 16 shows that the adsorbate, as prepared, was essentially pure. An additional proof of the purity is that the XPS spectra obtained on Pd(110) at 107 K display an approximately 2 to 1 N:C intensity ratio, as expected for molecularly adsorbed diazirine. It was difficult to accurately measure the actual exposure of the Pd(110) to diazirine. Very low apparent exposures as measured using the ion gauge yielded substantial submonolayer surface coverages of pure diazirine as measured by XPS. The XPS data were treated using commercial software. Good fits were obtained by using the Gaussian-Lorentzian product function. The background signal intensity as recorded on the clean Pd surface in the $N_{(1s)}$ and $C_{(1s)}$ regions for each experiment was subtracted from the recorded spectrum. The small amount of any remaining background was removed by a polynomial or linear background fit. Typical widths of the deconvoluted peaks were in the range 1.3–1.5 eV while the widths of the broad $N_{(1s)}$ peaks due to two dissimilar N atoms in a single species were of the order of 2.2 eV.

Results

XPS Measurements. XPS $N_{(1s)}$ data for diazirine adsorbed on Pd(110) are shown in Figure 2. The spectra obtained on adsorption at 107 K are split into two broad regions, one above 400 eV binding energy and one below. The best fit to the observed $N_{(1s)}$ spectra is obtained, as shown in Figure 2a, by placing one broad peak (fwhm = 2.3 eV) at 402.1 eV, a broad peak (fwhm = 2.2 eV) at 399.5 eV, and a narrow peak (fwhm = 1.3 eV) at 398.3 eV. However, as shown in Figure 2b, the feature above 400 eV is sufficiently broad to be arbitrarily resolved into two peaks of roughly equal intensity at 402.6 and 401.6 eV, respectively. The variation in intensity of the latter two peaks as a

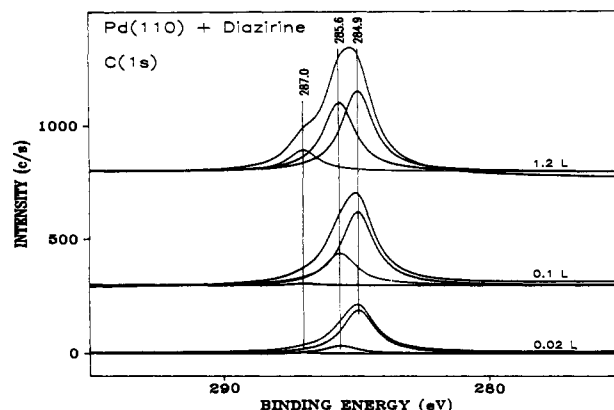


Figure 4. $C_{(1s)}$ spectra for diazirine adsorbed on Pd(110) at low ($\sigma_c = 1.9 \times 10^{14}$ atoms cm^{-2}), intermediate ($\sigma_c = 4.2 \times 10^{14}$ atoms cm^{-2}), and high surface coverage.

function of exposure, Figure 3, and of anneal temperature (data shown below), and as a function of photon irradiation,²⁹ shows conclusively that the observed width of the 402.1-eV feature arises from inequivalent nitrogens in a single state of molecularly adsorbed CH_2N_2 . In all instances the component peaks at 402.6 and 401.6 eV display the same functional dependence as one would expect for two atoms in a single adsorbed species. The data in Figure 3 also indicate that the $N_{(1s)}$ peaks above 400 eV are not satellites of the lower energy features, as satellite structure would be anticipated at all coverages. Satellite structure of comparable intensity to the main peak is observed in the case of molecular nitrogen adsorbed end-on on metal surfaces.²³ Partial screening of the $N_{(1s)}$ photoemission core hole is proposed to occur through charge transfer from the metal to the $\text{N}_2 \pi^*$ orbital.²³ However, in the case of diazirine, as pointed out by Yamabe et al.,⁷ the N_2 moiety is side-on bonded to the CH_2 group. The $\text{CH}_2 \rightarrow \text{N}_2 \pi^*$ charge transfer implicit in the latter mode of bonding is probably responsible for the fact that no satellite, unscreened final state structure is observed in the $N_{(1s)}$ spectra of adsorbed diazirine. The feature below 400 eV binding energy is clearly a convolution of at least two peaks and may be resolved to yield features located at 399.5 and 398.3 eV, indicating that at least two distinct species contribute intensity in the region below 400 eV. For the purposes of discussion we label the adsorbed state of diazirine which contributes $N_{(1s)}$ intensity above 400 eV as the γ -state, and we assume that two other states labeled α and β contribute intensity below 400 eV. We associate the α -state with the $N_{(1s)}$ peak at 398.3 eV. Figure 3 shows that the α - and β -states grow in first at lower coverage. With increasing exposure the γ -state is progressively populated and there is an increase in signal associated with the β -state (399.5 eV). Adsorption at low temperature, 107 K, leads to a nitrogen to carbon ratio which averages out over many experiments to 1.8:1 which is close to the value of 2:1 expected for molecular adsorption of CH_2N_2 . The observed 10% discrepancy may be due to error introduced during background subtraction from the broad $N_{(1s)}$ envelope which is superimposed on a sloping Pd background. The actual ratio for the spectra shown in Figure 3 is 2.1 N:1.0 C. As discussed below, diazirine dissociates on Pd(110) to yield N_{ads} and $\text{CH}_{2\text{ads}}$ species which display binding energies in the range 397.4–396.9 and 284.1–283.6 eV, respectively. The absence of features in these binding energy ranges on exposure to diazirine at 107 K indicates that the ad-

(23) Freund, H.-J.; Messmer, R. P.; Kao, C. M.; Plummer, E. W. *Phys. Rev.* **1985**, *B31*, 4848.

(24) Gambi, A.; Winnewisser, M.; Christiansen, J. J. *J. Mol. Spectrosc.* **1983**, *98*, 413.

(25) Kordesch, M. E.; Stenzel, W.; Conrad, H. *Surf. Sci.* **1986**, *175*, L687.

(26) Scofield, J. H. *J. Electron Spectrosc. Relat. Phenom.* **1976**, *8*, 129.

(27) Lindquist, J. M.; Ziegler, J. P.; Hemminger, J. C. *Surf. Sci.* **1989**, *210*, 27.

(28) Loggenberg, P. M.; Carlton, L. C.; Copperthwaite, R. G.; Hutchings, G. J. *Surf. Sci.* **1987**, *184*, L339.

(29) Mc Breen, P. H.; Serghini Monim, S. Submitted for publication in *Chem. Phys. Lett.*

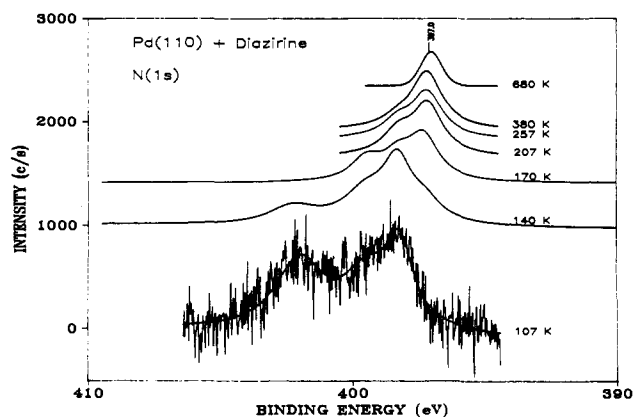


Figure 5. $N_{(1s)}$ spectra as a function of anneal temperature over the range 100–700 K for diazirine on Pd(110).

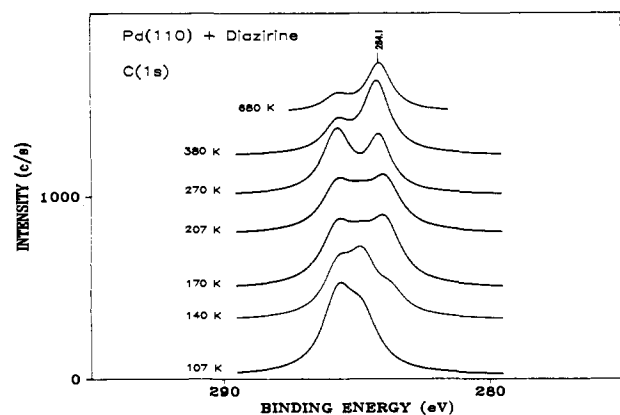


Figure 6. $C_{(1s)}$ spectra as a function of anneal temperature over the range 100–700 K for diazirine on Pd(110).

sorption is associative at low temperatures. As discussed above in the Experimental Section, the adsorbate introduced to the surface is itself pure. Thus we feel that essentially the entire $N_{(1s)}$ envelope of peaks at 107 K may be attributed to adsorbed molecular CH_2N_2 . Note that some of the CH_2N_2 species could possibly be present on the surface as diazomethane as well as in the form of diazirine if the gas–metal interaction induces ring opening. The possibility that some cyclic-to-linear isomerization occurs is considered in the Discussion Section. The equivalent $C_{(1s)}$ spectra as a function of exposure of diazirine to Pd(110) at 107 K are shown in Figure 4. The $C_{(1s)}$ spectra consist of a single broad feature which we resolve into two peaks at 285.6 and 284.9 eV, respectively. However, since the $N_{(1s)}$ spectra indicate that three different species are present on the surface at 107 K and since the $C_{(1s)}$ spectrum is a single broad peak, the two $C_{(1s)}$ peaks obtained on deconvolution should only be taken as a rough guide to the actual composition of the $C_{(1s)}$ spectrum. Intensity grows in at 285.6 eV as the γ -state is populated. The results of thermal annealing experiments also show that the 285.6-eV $C_{(1s)}$ peak belongs to the γ -state. A weak additional high binding energy, 287.0 eV, $C_{(1s)}$ feature is observed in some spectra and may be due to a small amount of condensed diazirine or more probably to an adsorbed impurity.

A general outline of the changes in, and redistribution of, $N_{(1s)}$ and $C_{(1s)}$ intensities as a function of anneal temperature is shown in Figures 5 and 6, respectively. Several important points should be noted. The $N_{(1s)}$ intensity decreases by approximately 70% in the region 107–207 K. A less pronounced decrease (40%) occurs in the $C_{(1s)}$ intensity. The γ - $N_{(1s)}$ state is almost completely removed at 140 K. Two new peaks emerge and dominate their respective spectra at 170 K. The new $N_{(1s)}$ peak appears at 397.3 eV and the new $C_{(1s)}$ feature appears at 283.6 eV. It is very important to note that the new $C_{(1s)}$ peak is present at 140 K whereas the new $N_{(1s)}$ feature is not. The formation of the new $N_{(1s)}$ peak coincides with a decrease in the intensity associated

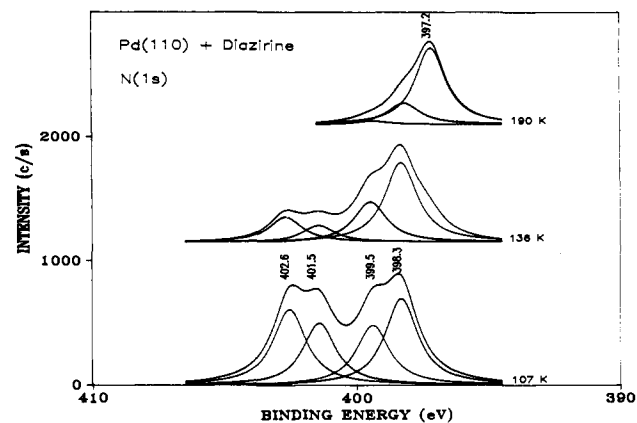


Figure 7. $N_{(1s)}$ spectra of diazirine adsorbed on Pd(110) as a function of anneal temperature over the low temperature range in which CN and NN bond cleavage occurs.

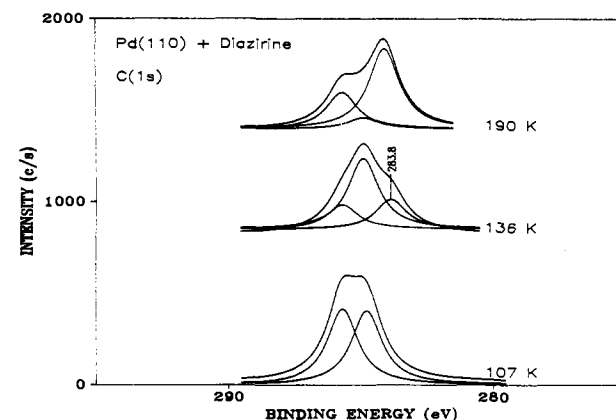


Figure 8. $C_{(1s)}$ spectra of diazirine adsorbed on Pd(110) as a function of anneal temperature over the low temperature range in which CN and NN bond cleavage occurs.

with the α - and β -states of adsorbed diazirine. Clearly both desorption and decomposition to adsorbed molecular fragments occur in the temperature range 107–207 K. The carbon to nitrogen atomic ratio is approximately 1:1 at 270 K. The $C_{(1s)}$ and $N_{(1s)}$ signals at 285.6 and 398.3 eV, respectively, do not go to zero on increasing the temperature to 270 K. We argue in the Discussion Section that the latter two features, at 270 K, arise from decomposition products of adsorbed molecular diazirine which are formed during annealing. Both of these features decay to zero over the temperature range 300–450 K, a change which is accompanied by a HCN desorption rate maximum in TPD measurements (data given below). A shift in binding energy of both the $N_{(1s)}$ and $C_{(1s)}$ low binding energy features occurs on thermal annealing. The $C_{(1s)}$ feature which originally displays a binding energy of 283.6 eV shifts toward 284.2 eV as the sample is annealed. This shift coincides with the emergence of the $N_{(1s)}$ feature at 397.3 eV. The latter feature shifts to lower binding energy as the temperature is raised and is found at 396.9 eV at 600 K. A more detailed series of spectra as a function of anneal temperature in the region 107–190 K are shown in Figures 7 and 8 for the $N_{(1s)}$ and $C_{(1s)}$ regions, respectively. The latter spectra illustrate a central observation; a lower anneal temperature is required to cause the emergence of the $C_{(1s)}$ feature at 283.6 eV than is required to cause the emergence of the $N_{(1s)}$ feature at 397.3 eV. All of our measurements show, as do the results displayed in Figure 7, that annealing the sample to approximately 130 K results in the almost total removal of the γ - $N_{(1s)}$ peaks. This change is accompanied by the appearance of a peak at 283.6 eV in the $C_{(1s)}$ spectrum and a reduction in intensity at 285.6 eV. However, it is necessary to anneal the sample to approximately 150 K to obtain a distinct low binding energy $N_{(1s)}$ peak at 397.3 eV. The growth of the latter feature is accompanied by a decrease in intensity of the α - and β - $N_{(1s)}$ features. The $N_{(1s)}$ peak at 399.5 eV is es-

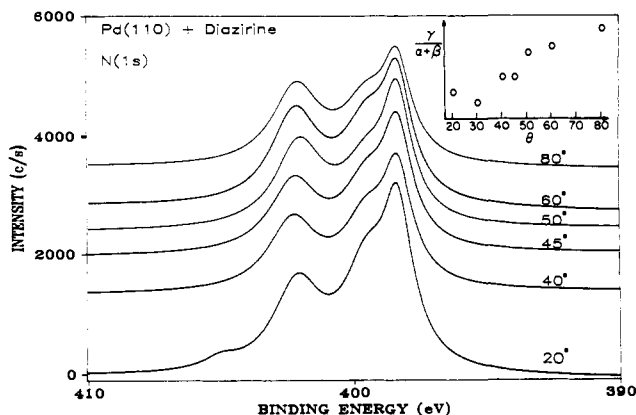


Figure 9. $N_{(1s)}$ spectra of diazirine adsorbed on Pd(110) as a function of the take-off angle. The ratio of the intensity of the γ -peak to the total intensity of the α - and β -peaks, as a function of the take-off angle, is given in the inset.

essentially removed on heating to approximately 200 K. The results shown in Figures 5 and 6 are for relatively high surface coverage of diazirine on Pd(110). For lower exposures, such that the ratio of the integrated $N_{(1s)}$ intensity above 400 eV is equal to or less than 0.5 of that below 400 eV, the decrease in the total $C_{(1s)}$ signal over the region 107–207 K is approximately 20%. The corresponding decrease in the total $N_{(1s)}$ intensity is approximately 70%.

As shown in Figure 9, it is evident that the $N_{(1s)}$ spectra display a marked angle of analysis dependent behavior. The intensity in the γ - $N_{(1s)}$ feature relative to the $N_{(1s)}$ intensity distributed below 400 eV is markedly greater at large angles, defined with respect to the surface plane, than at angles such as 20–40°. The fact that we can ratio one $N_{(1s)}$ envelope against another provides an efficient means of minimizing instrumental factors as a source of the observed angular dependence. The ratio of the peak areas of the γ -state with respect to the sum of the areas of the α - and β -states as a function of take-off angle is shown in the inset of Figure 9. The $C_{(1s)}$ spectra do not display an angular dependence.

Temperature-Programmed Desorption and Vibrational Spectroscopy Data. The thermal desorption data for diazirine adsorbed on Pd(110) are relatively complex. Data obtained at high and at low coverages of diazirine are shown in Figures 10 and 11, respectively. A number of significant features are common to all of the recorded spectra. A weak nitrogen desorption peak is observed in the region 600–700 K. This observation correlates with the removal at ≥ 600 K of $N_{(1s)}$ intensity at 396.9 eV as indicated in Figure 5. The $N_{(1s)}$ peak at 396.9 eV is removed completely on heating above 700 K. A feature at approximately 350 K for masses 26 and 27, but not for mass 28, indicates the desorption of HCN. This conclusion is supported by the observation (Figure 5) of a decrease in the $N_{(1s)}$ intensity at 398.4 eV in the region 300–450 K. As discussed below, the latter $N_{(1s)}$ peak is attributed to an adsorbed H_2CN species. The hydrogen desorption spectrum contains a peak at approximately 380 K and a broad tail which extends to temperatures above 600 K. The latter tail is characteristic of the gradual dehydrogenation of surface carbon species. All of the results display a striking difference between the m/e 42 spectrum, corresponding to the parent ion, and the m/e 14 spectrum corresponding to the most abundant ion. The latter spectrum contains an additional peak just above 200 K in each case. This mass 14 peak is accompanied by a simultaneous desorption rate maximum for masses 28, 2, and 16. The features are well resolved for desorption measurements involving low coverages and heating rates of 5 K/s, such as displayed in Figure 11. At high exposures, the m/e 28 peak is due to both C_2H_4 and N_2 desorption whereas only N_2 desorption is observed at low exposures. The latter conclusion is based on a comparison of m/e 28, 27, and 26 desorption traces. The spectra shown in the lower panels of Figures 10 and 11 were obtained by subtracting out the contributions of N_2 , CH_4 , CH_2N_2 , and C_2H_4 , in the case of high surface coverage (Figure 10), from the measured m/e 14 signal. Further details on the data treatment involved are given

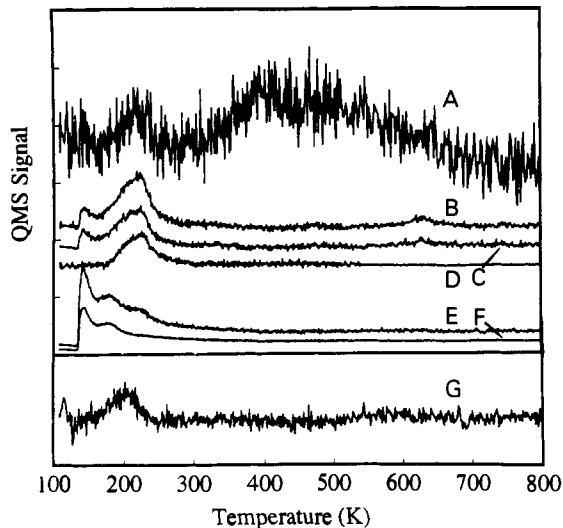


Figure 10. Thermal desorption spectra for high coverage of diazirine on Pd(110) with a heating rate equal to 0.5 K/s and the magnification factors given in parentheses: m/e 2 ($\times 10$) (A), 28 ($\times 2$) (B), 27 ($\times 2$) (C), 16 ($\times 2$) (D), 14 ($\times 1$) (E), 42 ($\times 5$) (F). The lower panel, spectrum G, shows the signal which remains on subtracting out the contribution of C_2H_4 , CH_4 , N_2 , and CH_2N_2 to the m/z 14 trace. The resultant spectrum is magnified by a factor of 2.

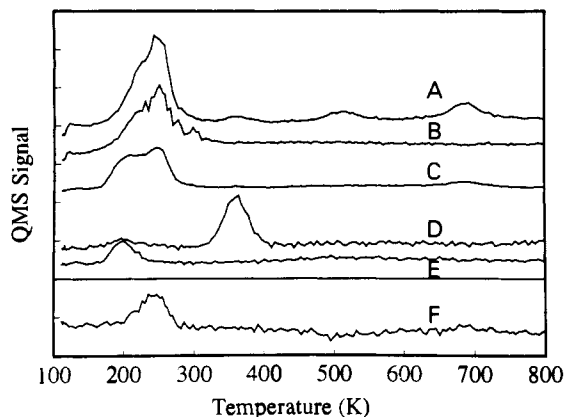


Figure 11. Thermal desorption spectra for low coverage of diazirine on Pd(110) with a heating rate equal to 5 K/s: m/e 28 ($\times 1$) (A), 16 ($\times 1$) (B), 14 ($\times 1$) (C), 26 ($\times 15$) (D), 42 ($\times 10$) (E). The lower panel, spectrum F, shows the m/e 14 trace following removal of contributions from CH_4 , N_2 , and CH_2N_2 . The latter spectrum is magnified by a factor of 2.

elsewhere.³⁶ The peaks corresponding to molecular desorption of diazirine are, of course, present in both the mass 42 and the mass 14 spectra. A single molecular desorption peak at approximately 190 K was observed for all the low coverage measurements. Figure 10 shows that an additional molecular desorption peak grows in quite strongly at approximately 125 K for high exposure of Pd(110) to diazirine at 107 K. Closer inspection of the mass 28 and mass 16 features which peak above 200 K indicates that there is a low temperature shoulder at approximately 180 K (Figure 10), in addition to a contribution (in the case of mass 28) from the cracking of molecular desorbed diazirine. The shoulders in the mass 16 and mass 28 spectra are clearly resolved

(30) Steinbach, F.; Kiss, J.; Krall, R. *Surf. Sci.* **1985**, *157*, 401.

(31) Levis, R. J.; DeLouise, L. A.; White, E. J.; Winograd, N. *Surf. Sci.* **1990**, *230*, 35.

(32) Ceyer, S. T. *Langmuir* **1990**, *6*, 82.

(33) Mc Breen, P. H.; Serghini Monim, S. Accepted for publication in *Surf. Sci.*

(34) Berlowitz, P.; Yang, B. L.; Butt, J. B.; Kung, H. H. *Surf. Sci.* **1985**, *159*, 540.

(35) Burke, M. L.; Madix, R. J. *J. Am. Chem. Soc.* **1991**, *113*, 105.

(36) Serghini Monim, S.; Mc Breen, P. H. Accepted for publication in *J. Phys. Chem.*

in Figure 11, where they are observed to fall between the two mass 14 desorption maxima. In total, the thermal desorption results show that diazirine has a rich chemistry on Pd(110) which involves the rupture of both CN and NN bonds, the formation of methane, ethylene, and HCN, and the desorption of a fragment which gives a strong mass 14 peak. Preliminary results obtained using electron energy loss spectroscopy are mentioned simply in order to serve as a check on the consistency of our interpretation of the more complete set of XPS and TPD data. A low coverage of diazirine on Pd(110) at 90 K results in a spectrum displaying intense losses at 2952, 1420, and 984 cm^{-1} . The A_1 modes of gas-phase diazirine occur at 3025 cm^{-1} , (CH_2)_s; 1623 cm^{-1} , $\nu(\text{NN})$; 1459 cm^{-1} , δ -(CH_2); and 992 cm^{-1} , $\nu(\text{CN})$ _s, respectively.²⁴ Warming the surface to 170 K results in the emergence of an intense electron energy loss at 1920 cm^{-1} and in a significant change in the relative intensities of the two low frequency losses when compared to the spectrum at 90 K. The feature at 1920 cm^{-1} is removed on heating to room temperature. The latter result indicates that the loss at 1920 cm^{-1} is not due to adsorbed CO.

Discussion

The discussion of the experimental results will be separated into three sections. First, the data will be analyzed in order to ascertain the various bond-breaking steps which occur during thermal decomposition of diazirine on Pd(110). The second section will concern the characterization of the various adsorbed states of diazirine which are present on Pd(110) at 107 K. In the third section, we will seek to rationalize the selective activation of the CN or NN bonds in terms of the modes of bonding of molecular diazirine to the surface at 107 K.

A. Thermal Decomposition: XPS and TPD Data. Temperature-programmed desorption results, such as shown in Figures 10 and 11, display a weak molecular nitrogen desorption peak in the region 600–700 K indicative of the recombinative desorption of atomic nitrogen. The XPS $N_{(1s)}$ data confirm the presence of atomic nitrogen on the surface. As indicated in Figure 5, an $N_{(1s)}$ feature at 396.9 eV is clearly resolved for a diazirine exposed surface which is annealed to 680 K. An $N_{(1s)}$ binding energy of 396.9 eV is characteristic of adsorbed atomic nitrogen.⁴⁷ In fact, $N_{(1s)}$ intensity in the region characteristic of N_{ads} emerges for temperatures as low as 150 K at which point a feature at 397.3 eV develops. The $N_{(1s)}$ intensity at 396.9 eV disappears between 600 and 700 K consistent with the TPD spectra which show N_2 desorption in the same region. The detection of adsorbed atomic nitrogen by both TPD and XPS measurements is proof that a fraction of adsorbed diazirine on Pd(110) undergoes NN bond cleavage. The deposition of a certain concentration of nitrogen adatoms might be expected to lead to the deposition of an equivalent quantity of adsorbed $\text{CH}_2\text{N}_{\text{ads}}$, or a decomposition product of a transient $\text{CH}_2\text{N}_{\text{ads}}$ species, on the surface. NN bond cleavage in the interaction of diazirines with iron carbonyls¹¹ leads to a product in which a R_2CN ligand is bridge bonded across two iron atoms such as shown in Figure 12D.¹¹ Evidence for a dissociative reaction of the type $\text{CH}_2\text{N}_2/\text{Pd}(110) \rightarrow \text{CH}_2\text{N}_{\text{ads}} + \text{N}_{\text{ads}}$ is provided in both the TPD and the XPS results. The TPD spectra display a HCN desorption peak at 350 K which is the temperature range characteristic of HCN desorption from metal

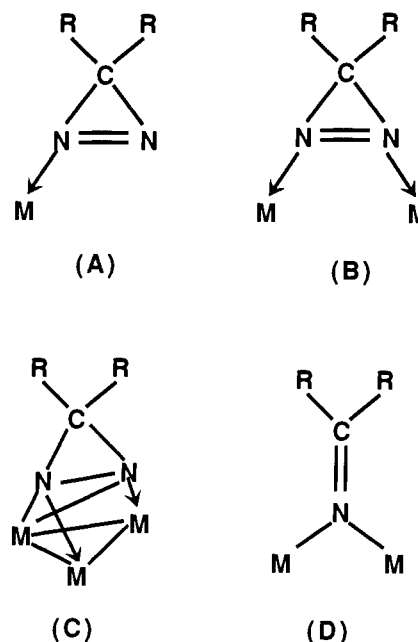


Figure 12. Schematic representation of the structure of diazirine-metal compounds as taken from the work of Kisch et al.¹¹

surfaces.²⁵ We assume that the hydrogen cyanide results from the partial dehydrogenation of an adsorbed CH_2N species. The XPS spectra taken in the temperature region 190–300 K display a persistent $N_{(1s)}$ peak at 398.4 eV and a persistent $C_{(1s)}$ peak at 285.6 eV. Furthermore, as indicated in Figures 5 and 6, the latter two peaks are removed simultaneously on annealing to approximately 400 K. Thus we attribute the two features to a single adsorbed species which yields the HCN thermal desorption peak at 350 K. At 225 K, the atomic nitrogen to carbon ratio, calculated by applying the Scofield photoionization cross section values^{26,51} to the normalized peak areas of the 398.4- and 285.6-eV features, averages to close to 1:1 as anticipated for a species such as $\text{H}_2\text{CN}_{\text{ads}}$. Similarly, at 225 K the $N_{(1s)}$ intensity at approximately 397.1 eV is roughly equal to the $N_{(1s)}$ intensity at 398.4 eV consistent with an equivalent amount of adsorbed N and CH_2N species. The observed $C_{(1s)}$ and $N_{(1s)}$ binding energies of 285.6 and 398.4 eV are not inconsistent with the presence of adsorbed CH_2N . The $N_{(1s)}$ and $C_{(1s)}$ binding energy of such a species depends strongly on whether bonding with the surface occurs solely through the nitrogen lone pair or whether both carbon and nitrogen interact with the surface.²⁷ The relatively high $N_{(1s)}$ binding energy of 398.4 eV indicates that bonding does occur solely via the nitrogen atom. Nitrogen-bonded HCN on Pt(111) is characterized by a peak at 398.6 eV,²⁷ and linear CH_2N_2 adsorbed on Fe is characterized by a $C_{(1s)}$ peak at 285.5 eV.²⁸ Thus, we assign the observed features at 398.4 and 285.6 eV to N-bonded $\text{CH}_2\text{N}_{\text{ads}}$.

Both the TPD and the XPS results provide strong evidence that a fraction of the adsorbed diazirine also decomposes through selective breaking of the CN bonds. This decomposition route yields adsorbed methylene, or species derived from CH_2 , and the desorption of molecular nitrogen. As indicated in Figures 5 and 6, slight annealing to approximately 140 K, following adsorption of diazirine at 107 K, leads to the transfer of $C_{(1s)}$ intensity into the low binding energy region and to the removal of most of the $\gamma\text{-N}_{(1s)}$ intensity. The new $C_{(1s)}$ peak occurs at 283.6 eV. In a separate set of experiments,²⁹ we have observed that photon irradiation of diazirine exposed Pd(110), using a Hg arc lamp as a broadband source, also results in the emergence of a $C_{(1s)}$ feature at 283.6 eV coincident with the removal of $\gamma\text{-N}_{(1s)}$ intensity. In

(37) Domen, K.; Chuang, T. J. *J. Am. Chem. Soc.* **1987**, *109*, 5288.

(38) Serafin, J. G.; Friend, C. M. *J. Am. Chem. Soc.* **1989**, *111*, 8967.

(39) Smentkowski, V. S.; Cheng, C. C.; Yates, J. T., Jr. *Surf. Sci.* **1989**, *215*, L279.

(40) Menu, M. J.; Desrosiers, P.; Dartiguenave, M.; Dartiguenave, J.; Bertrand, G. *Organometallics* **1987**, *6*, 1822.

(41) Hoffmann, R. *Tetrahedron* **1966**, *22*, 539.

(42) Kuwahara, Y.; Jo, M.; Tsuda, H.; Onchi, M.; Nishijima, M. *Surf. Sci.* **1987**, *180*, 421.

(43) Egelhoff, W. F., Jr. *Surf. Sci.* **1984**, *141*, L324.

(44) Martensson, N.; Nilsson, A. *J. Electron Spectrosc. Relat. Phenom.* **1990**, *52*, 1.

(45) Petersson, L. G.; Kono, S.; Hall, N. F. T.; Fadley, C. S.; Pendry, J. *B. Phys. Rev. Lett.* **1979**, *42*, 1545.

(46) Wesner, D. A.; Coenen, F. P.; Bonzel, H. P. *Phys. Rev.* **1989**, *B39*, 10770.

(47) Grunze, M.; Golze, M.; Hirschwald, W.; Freund, H.-J.; Pulm, H.; Seip, U.; Tsai, M. C.; Ertl, G.; Kuppers, J. *Phys. Rev. Lett.* **1984**, *53*, 850.

(48) Nishijima, M.; Yoshinobu, J.; Sekatani, T.; Onchi, M. *J. Chem. Phys.* **1989**, *90*, 5114.

(49) Demuth, J. E. *Surf. Sci.* **1980**, *93*, 127.

(50) Stroschio, J. A.; Bare, S. R.; Ho, W. *Surf. Sci.* **1984**, *148*, 499.

(51) Carley, A. F.; Roberts, M. W. *Proc. R. Soc. London* **1978**, *A363*, 403.

the latter case we attribute the peak at 283.6 eV to adsorbed methylene resulting from the photon-induced dissociation of diazirine, since gas-phase photolysis of diazirine is known to yield :CH_2 and N_2 . A binding energy of 283.6 eV is 1.2 eV lower than the value previously attributed to adsorbed methylene, as obtained through the decomposition of CH_2Cl_2 on Co ,³⁰ but is in the range one might expect for C_{1s} species.³¹ This discrepancy may simply be due to the difficulty inherent in preparing isolated methylene adspecies. Halocarbon precursors lead to halogen coadsorption, and consequently to both initial and final state effects, and hydrocarbon precursors such as C_2H_4 lead to complex dissociation pathways. Highly reactive species such as unsaturated hydrocarbon fragments are susceptible to reaction with each other or with free surface to give species which are ill defined even though they may contain functional groups such as CH_2 , CH , or CH_3 . Thus the $\text{C}_{(1s)}$ binding energy for isolated CH_2 groups may well be different from that of a partially hydrogenated carbon deposit of general formula $(\text{CH}_2)_x$ or of CH_2 adsorbed in the proximity of Cl_{ads} , for example. A case in point is the EELS study of CH_3 and CH species on $\text{Ni}(111)$ by Ceyer et al.³² which reveals that the vibrational spectra of isolated CH_3 and CH species produced via methane activation are quite different from those of CH_3 and CH groups formed through the thermal decomposition of adsorbed hydrocarbons, or through the decomposition of halocarbons, for example. A full discussion of the assignment of 283.6 eV as the $\text{C}_{(1s)}$ binding energy for CH_2 on $\text{Pd}(110)$ is given elsewhere.³³ The TPD results provide indirect evidence for the presence of CH_2 species on the surface. The desorption of both methane and ethylene is clearly observed as shoulders at approximately 180 K in Figure 10. We propose that methane is formed through the interaction of CH_2 groups with adsorbed hydrogen. This could either be hydrogen which is abstracted by the surface from diazirine or from adsorbed CH_2 . Ethylene may be formed through the dimerization of CH_2 units. Note that ethylene formation only occurs for high initial exposures of diazirine (Figure 10). Hydrogenation to methane or dehydrogenation to surface carbon is favored over dimerization at low surface coverages (Figure 11). The chemistry which we observe for methylene on $\text{Pd}(110)$ is very similar to that reported by Berlowitz et al.³⁴ for methylene on $\text{Pt}(111)$. Note that a shift in binding energy, from 283.6 eV toward 284.0 eV, occurs on annealing the sample above 150 K. We propose that this shift arises through the deposition of atomic nitrogen at these temperatures and through the interaction of CH_2 adspecies to form a carbonaceous residue which remains on the surface to high temperatures.³³

It is important to note that the XPS $\text{C}_{(1s)}$ data indicate that adsorbed methylene is formed on annealing the surface to only 130 K (Figure 8), whereas the $\text{N}_{(1s)}$ data show that further annealing, to ≥ 150 K (Figure 7), is required to generate an $\text{N}_{(1s)}$ feature in the region of 397.3 eV characteristic of atomic nitrogen. There is a further growth in the intensity of the $\text{C}_{(1s)}$ feature characteristic of CH_2 , or CH_2 derived species, above 150 K. These combined results indicate that a decomposition process limited to CN bond breaking occurs at very low temperatures whereas both CN and NN bond breaking events occur above 150 K. As discussed below, the low-temperature region, 107–140 K, corresponds to the removal of the adsorbed γ -state of diazirine and the region above 150 K corresponds to the decomposition the β - and α -states of adsorbed diazirine. The fact that CH_4 and C_2H_4 desorption does not occur until ≥ 170 K (Figure 10) may simply be due to the activation energy necessary for the required reactions or to the need of a sufficient concentration of reactants on the surface. However, it may also be related to competition for surface sites resulting from the NN bond breaking reaction above 150 K which deposits atomic nitrogen and H_2CN , or species derived from H_2CN , on the surface. There have been a number of recent reports of how coadsorbed species such as CO favor bond making reactions in hydrocarbon surface chemistry.³⁵

A most intriguing aspect of TPD spectra shown in Figures 10 and 11 is the fact that above 200 K an intense peak at mass 14 is detected in the absence of a peak at 42 corresponding to the diazirine parent ion. Furthermore, the mass 14 peak is accom-

panied by a desorption signal for masses 16 and 28. However, the fragmentation corrected spectra displayed in the lower panels of Figures 10 and 11 show that the mass 14 peak is too intense to be accounted for in terms of the cracking of species such as N_2 , C_2H_4 , or CH_4 . These results provide strong evidence for the direct generation of gas-phase methylene through the thermal decomposition of CH_2N_2 on the surface.³⁶ Such a process could also liberate N_2 , CH_4 , and C_2H_4 through interaction of some of the released methylene diradical with either the surface or the chamber walls. In fact coincident detection of ethylene, methane, and methylene occurs for high initial coverages of diazirine such as shown in Figure 10. Ethylene is not observed for low initial coverages of diazirine (Figure 11). The desorption of a radical from a metal surface is not an expected observation in surface chemistry studies, although there are some precedents for such a phenomenon. Domen and Chuang³⁷ reported the thermal desorption of methylene from a CH_2I_2 -exposed Al polycrystalline disk. Serafin and Friend³⁸ have reported the generation of gas-phase CH_3 in thermal desorption measurements of methoxy species on oxygen exposed $\text{Mo}(110)$. The desorption of the :CCl_2 diradical was observed by Smentkowski et al.³⁹ during a study of the adsorption of CCl_4 with $\text{Fe}(110)$. As discussed elsewhere, the most probable mechanism for the formation of gas-phase methylene from adsorbed diazirine is via ring opening to obtain an adsorbed diazomethane intermediate.³⁶ Such an intermediate is supported by preliminary EELS data. An electron energy loss is observed at 1920 cm^{-1} when low coverage of diazirine is warmed to 170 K. A vibrational frequency in this region is diagnostic of the NN stretching of an azo ligand group bonded to a metal center.⁴⁰ This mode of bonding, with the NNC axis roughly perpendicular to the surface, leads to the formation of gas-phase methylene through the rupture of the CN bond and the formation of the extremely stable N_2 molecule. Bonding to the surface activates this process in that the chemisorption bond is formed by removing electron density from the HOMO orbital which is bonding in CN and antibonding in NN,⁴¹ thereby advancing the molecule along a reaction coordinate in which the CN bond is weakened and the NN bond is strengthened. The end result is coincident :CH_2 ejection and N_2 desorption, as molecular nitrogen has a negligible residence time on $\text{Pd}(110)$ at temperatures above 200 K.⁴² This analysis assumes that the observed free methylene does not interact directly with the surface during the ejection process and that the process is analogous to the gas-phase thermolysis of diazirine. A detailed discussion of the mechanism by which the activation energy for the release of methylene into the gas phase is surmounted is given elsewhere.³⁶

B. Adsorbed States of Diazirine on Pd(110) at 107 K. The integrated $\text{N}_{(1s)}$ and $\text{C}_{(1s)}$ intensities observed on adsorption at 107 K show that the C:N ratio is close to 2:1 as expected for the molecular adsorption of CH_2N_2 . However, the presence of a number of distinct chemisorbed states may be directly inferred from the spread in the $\text{N}_{(1s)}$ binding energies, such as that displayed in Figure 2. The γ -state, which grows in above 400 eV at high coverage (Figure 3), is sufficiently broad to be arbitrarily deconvoluted to yield two $\text{N}_{(1s)}$ peaks of roughly equal intensity at approximately 402.6 and 401.6 eV. Temperature-dependence measurements (Figure 5) show that this state corresponds to a single adsorbed species since all of the intensity is removed simultaneously on heating. Furthermore, the width of the feature (Figure 2) indicates that the species contains two inequivalent nitrogens displaying binding energies separated by approximately 0.8–1.0 eV. This separation is reminiscent of the binding energy separation of 1.2 eV which exists for the inner and the outer nitrogen atoms of adsorbed molecular nitrogen on $\text{Ni}(100)$ ⁴³ and suggests an adsorbed species in which diazirine is chemisorbed in an on-top site via one of the nitrogen atoms, such as indicated by structure I shown in Figure 13. The width of the γ -feature centered at 402.1 eV, fwhm of approximately 2.3 eV, is also the same as that observed for the screened $\text{N}_{(1s)}$ state of N_2 on $\text{Ni}(100)$.^{43,44} The high binding energy is then partly due to the donor nature of the molecule-metal bond which decreases the electron density in the environment of the nitrogen atoms.

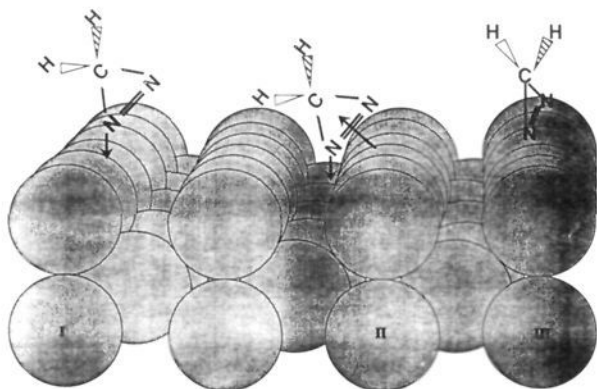


Figure 13. Proposed approximate adsorption geometries for diazirine adsorbed on Pd(110) at 107 K.

Further support for the proposed geometric configuration of the γ -state is provided by the results, shown in Figure 9, of measurements of the angular dependence of the $N_{(1s)}$ spectra made in the [001] direction. An angular dependence would arise from photoelectron diffraction effects wherein forward scattering causes the detected photoemission intensity to be enhanced at angles of analysis, with respect to the surface, which coincide with the angles made by the NN and NC bonds.⁴⁵ Diazirine is a highly symmetrical molecule with an NNC bond angle of 64.8° and is thus readily amenable to structure analysis using HREELS or angle-resolved XPS measurements. If the γ -state has an orientation similar to that depicted in structure I then it should show an enhancement of the $N_{(1s)}$ photoemission intensity related to the nitrogen closest to the surface for angles of analysis which correspond to the angles which the NC and NN bonds make with the surface plane. If we estimate the latter angles to be approximately 60° and 55° , respectively, then the γ -state $N_{(1s)}$ intensity should show a broad enhancement peak at high take-off angles. The typical width of a forward scattering feature is 20° at half maximum.⁴⁶ The set of spectra shown in Figure 9 display a marked increase in the γ -state $N_{(1s)}$ intensity relative to the $N_{(1s)}$ intensity below 400.0 eV as the angle of analysis increases. The ratio of the integrated peak areas, as shown in the inset of Figure 9, displays a sharp increase in the relative contribution of the γ -state for angles above 45° . Furthermore, insofar as we are able to deconvolute the broad peak at 402.1 eV, the γ -state component at 402.6 eV is more intense relative to the component at 401.6 eV at high take-off angles. This is consistent with an assignment, in analogy to the well-established case for adsorbed molecular nitrogen,⁴³ of the higher binding energy to the nitrogen atom which is bonded to the surface. Forward scattering by the outer nitrogen atom, and the carbon atom as well in the case of diazirine, causes enhancement, at the appropriate angles, of the detected photoemission from the inner nitrogen. The angular dependence XPS measurements do not enable us to estimate the exact value of the angle between the NN bond and the surface plane. However, the results provide a clear indication that the NN bond is tilted strongly with respect to the surface, the angle being greater than 45° . Furthermore, there need not necessarily be a unique angle for the NN bond with respect to the surface. The γ -state is progressively populated at higher coverages and is adsorbed in the presence of the species which yield $N_{(1s)}$ intensity below 400 eV. Wesner et al.⁴⁶ have used photoelectron diffraction measurements to show that CO adsorbed on Pt(111) tilts by 20° at high coverage from the upright configuration which it adopts at low coverage. Similarly, diazirine, depending on its local environment, may display a range of NN-surface angles instead of the ideal angle adopted by an isolated molecule displaying structure I.

The angle-dependent $N_{(1s)}$ results discussed above and the γ - $N_{(1s)}$ peak line width suggest that the γ -state is highly tilted with respect to the surface. The same results also imply that the species contributing $N_{(1s)}$ below 400 eV are not tilted to any great extent. The ratio of the β -state (399.5 eV) to the α -state (398.3

eV) is relatively constant as a function of the angle of analysis, although a slight maximum at 30° is observed, and the combined intensity of the α - and β -states decreases relative to the γ -state as the take-off angle increases. As shown in Figure 3, the α -state is populated first and the β - and γ -states grow in as the exposure is progressively increased. The α -state corresponds to the molecularly adsorbed state of CH_2N_2 in which the nitrogen atoms are equivalent. However, as discussed above, the β -feature displays a broad $N_{(1s)}$ feature which indicates inequivalent nitrogens. One cannot rule out the possibility that the β -state is adsorbed diazomethane arising from ring opening of diazirine on Pd(110) at 107 K. However, EELS spectra do not support a ring opening reaction at low temperature and low surface coverage. The EELS measurements, albeit at 90 K in contrast to 107 K for the XPS measurements, display a spectrum consistent with diazirine adsorbed in a configuration displaying C_{2v} symmetry. As discussed in the previous section, the EELS results do indicate the formation of a diazomethane species on the surface on warming to 170 K.

The combined angle dependent, binding energy, and peak width data enable us to postulate different approximate adsorption geometries for diazirine on Pd(110) such as those shown in Figure 13. As a point of reference it is useful to consider the different ligand-metal bonding geometries observed for organometallic complexes of diazirine. The work of Kisch et al.¹¹ reveals that diazirines interact with $Fe_2(CO)_9$ to yield the types of products shown in Figure 12. Complexes A and B involve only σ -bonds with metal atoms, but complex C also involves π -bonding. For diazirine adsorbed on Pd(110) it is also necessary to consider the atomic structure of the surface which consists of rows of atoms separated by atomic troughs (Figure 13). Structure I, the highly tilted species characterized by a broad $N_{(1s)}$ peak at 402.1 eV and a $C_{(1s)}$ feature at 285.6 eV, primarily involves a σ -donor bond from nitrogen to a palladium atom. Metal-molecule back bonding is limited due to poor overlap between the π^* orbitals of the highly tilted NN bond and the metal d orbitals. The fact that the bonding is donor type and the fact that the molecule is weakly coupled to the surface results in the relatively high binding energy of 402.1 eV. The β - and α -states of diazirine on Pd(110) display much lower $N_{(1s)}$ binding energies, 399.5 and 398.4 eV, respectively. These binding energy values fall close to the value of 399.0 eV observed for π -bonded molecular nitrogen on Fe(111).⁴⁷ Substantial π -bonding between molecular diazirine and Pd(110) would require that the NN bond be oriented roughly parallel to the surface. However, on the atomic level this can be achieved in two fashions such as shown schematically in structures II and III displayed in Figure 13. The diazirine molecule could be oriented in structure III either along the Pd row atoms or along the palladium trough atoms. In both cases the two nitrogen atoms are equivalent and the $N_{(1s)}$ spectrum should display a narrow peak such as is observed at 398.4 eV. Structure II involves interaction with both trough and row atoms and hence it is slightly tilted with respect to the macroscopic surface plane. Such a structure has been proposed for acetylene adsorbed on both Pd(110)⁴⁸ and Ni(110).^{49,50} This structure involves inequivalent nitrogen atoms and would give rise to a broad $N_{(1s)}$ feature such as that observed at 399.5 eV. The question then arises as to why neither structure II nor structure III displays angle dependent variations in the $N_{(1s)}$ photoelectron intensity. However, the angle dependent measurements were made in the direction perpendicular to the rows of palladium atoms, the [001] direction. Thus, structures wherein the NN bond of diazirine is oriented in the [110] or [112] directions would not be expected to display angle dependent behavior under our experimental conditions. This analysis implies that structure II is bridge bonded between one row atom and one trough atom rather than along the [001] direction. It is also likely that diazirine adopting structure III would be aligned along, rather than perpendicular to, the atomic rows. The assumption is made that structure I permits free rotation of the adsorbed species. We wish to emphasize that the three structures given in Figure 13 are only intended to be taken as approximate representations of the actual structures which give rise to the three $N_{(1s)}$ peaks at 402.1, 399.5, and 398.4 eV, respectively. However, these schematic

structures do indicate the salient point that we may divide the three surface species into one (structure I) which involves negligible π -bonding to the surface and two (structures II and III) which involve substantial π -bonding to the surface. In other words, the proposed structures are used to indicate two significantly different modes of bonding between molecular diazirine and Pd(110). This important distinction was justified above on the basis of the observed $N_{(1s)}$ binding energies, the width of the $N_{(1s)}$ features, and the angular dependence of the $N_{(1s)}$ photoelectron signal. The proposed approximate structures are also in line with the intuitive idea that the first diazirine molecules to arrive at the surface (the α -state) adopt a configuration in which both nitrogen atoms of the symmetrical molecule are in contact with the surface. Then, as the surface coverage increases, states in which the NN bond is slightly tilted (the β -state) and finally fully tilted (the γ -state) are progressively filled. Further experimental evidence for structure III is given by preliminary HREELS data for low coverages of diazirine on Pd(110). The spectra taken at 90 K for low coverage of diazirine display all the expected A_1 modes of diazirine adsorbed in a C_{2v} configuration such as structure III, save the $\nu(\text{NN})$ stretching mode and the metal–molecule stretching mode.²⁴ However, the $\nu(\text{NN})$ loss is expected to be weak for such a structure as the NN bond is aligned parallel to the surface. As discussed below, further strong support for the proposed structures emerges in that the mode of decomposition of the various species is consistent with the form of metal–molecule bonding implicit for each proposed structure. In addition, the proposed approximate structures are not inconsistent with the diazirine–metal bonding geometries reported for organometallic complexes¹¹ and shown in Figure 12.

C. Adsorption Geometry Dependent Selective Bond Activation. $C_{(1s)}$ XPS measurements, such as those displayed in Figure 8, show that when the diazirine-exposed Pd(110) is warmed from 107 K to approximately 130 K a new $C_{(1s)}$ peak appears at 283.6 eV and intensity is removed from the 285.6-eV region. For the same temperature difference, the $N_{(1s)}$ feature corresponding to the γ -state decreases sharply in intensity whereas the $N_{(1s)}$ peaks below 400.0 eV remain relatively stable. Since a binding energy of 283.6 eV may be associated with adsorbed methylene, the overall result is that the γ -state can undergo CN bond breaking to yield adsorbed CH_2 and gas-phase N_2 . In a separate study²⁹ we have found that methylene deposition also occurs when a diazirine-exposed Pd(110) surface is subjected to Hg-arc lamp irradiation for a short period of time. Longer periods of irradiation result in a transformation of the α - and β -states to yield adsorbed nitrogen. Similarly, as discussed in section A, heating to 150 K causes surface decomposition of the α - and β -states resulting in an increase in the $C_{(1s)}$ signal at 283.6 eV and the emergence of an $N_{(1s)}$ peak at 397.3 eV (Figure 7) due to the deposition of atomic nitrogen. Thus, in summary, the γ -state selectively undergoes CN bond breaking and the α - and β -states undergo both CN and NN cleavage. Furthermore, CN bond scission commences at lower temperatures than that required for NN cleavage.

A rationalization for the specific bond activation associated with the various states of adsorbed diazirine may be obtained by considering the frontier orbitals of diazirine^{8,41} and the modes of bonding of the molecule with the surface. The highest occupied molecular orbital of diazirine, the $3b_2$ orbital, is bonding in CN and antibonding in NN. The lowest unoccupied molecular orbital, the a_2 orbital, may be regarded as a π^* NN antibonding orbital. The LUMO and HOMO orbitals are located in energy at approximately -7.5 and -11.5 eV, respectively.⁸ The latter values, which imply a high-lying donor state and a low-lying affinity level, suggest that as an adsorbate diazirine should display some similarities to CO which is a prototypical σ -donor, π -acceptor adsorbate. Thus in terms of energy match alone diazirine should behave like a good π -acceptor adsorbate. However, in terms of orbital overlap, CO is less demanding in that the $2\pi^*$ orbital is skewed toward the carbon end of the molecule whereas in the case of diazirine the π^* orbital is symmetric with respect to the plane bisecting the NN bond. Thus one would expect π bonding between diazirine and metal surfaces to be greatly favored in cases where

the NN bond lies roughly parallel to the surface in contrast to adsorption geometries in which the NN bond is tilted away from the surface.⁵² In structure I the NN bond is tilted away from the surface and the interaction with the surface is primarily a σ -type donor bond. Such a bonding configuration should result in an increase in the NN bond order and a decrease in the CN bond order due to the characteristics of the HOMO orbital as described above. The surface–molecule interaction in structure I, then, serves to advance the system along a reaction coordinate which ultimately results in the rupture of the CN bond, the generation of free molecular nitrogen, and the deposition of methylene on the surface as evidenced by a $C_{(1s)}$ peak at 283.6 eV. Structures such as II and III on the other hand permit significant overlap of the diazirine π orbitals with metal orbitals. Thus one could anticipate electron back donation into the low-lying π^* acceptor level of the molecule and consequent activation of the NN bond. A σ -donor bond component is also involved, and the CN bond will be activated too. In other words, bonding according to structures II and III would serve to advance the system along a reaction coordinate leading to NN bond cleavage and perhaps also some CN cleavage. The fact that the α - and β -states do decompose to yield adsorbed nitrogen as indicated by the $N_{(1s)}$ peak at 396.9 eV is further evidence that they correspond to adsorption geometries such as structure II or III in which the NN bond is activated. The above analysis also provides a means for understanding the apparently anomalous result that the γ -state of adsorbed diazirine dissociates prior to the α - and β -states. Normally, one assumes that the first state to be populated on a surface is the most strongly activated species and thus should be the most likely to dissociate. However, one must recall that diazirine provides two different bonds, the CN and the NN bond, which may be activated. Furthermore, diazirine is a strained molecule which contains latent molecular nitrogen and therefore has a tendency to dissociate under suitable conditions to yield the extremely strong nitrogen–nitrogen triple bond and the methylene diradical. The internal dynamics of the molecule can then, in response to activation through chemisorption, lead to such unanticipated results as the preferential dissociation of the third adsorption state to be populated or surface decomposition to yield free methylene. Chemisorption into structure I, which corresponds to the γ -state, activates the usual decomposition process for diazirine, that is the liberation of molecular nitrogen. Chemisorption into structures II and III, which correspond to the β - and α -states, respectively, weakens the NN bond of diazirine and therefore does not promote the usual decomposition process. Chemisorption into the latter states is strong enough to cause NN bond rupture at 150 K. However, structure I, despite its lower adsorption energy as indicated by the fact that it is the third state to populate, decomposes prior to structures II and III because of the intramolecular driving force toward the production of methylene and nitrogen. Thus, diazirine is an example of an adsorbate for which the surface chemistry may be qualitatively separated into processes driven by the metal surface and by the molecule itself.

Acknowledgment. Partial funding for this research has been provided by the Networks of Centres of Excellence in Molecular and Interfacial Dynamics, one of the fifteen Networks of Centres of Excellence supported by the Government of Canada. Funding for the project was also made available through an NSERC Operating Grant, an FCAR Equipe grant, and a University Research grant from Imperial Oil Ltd. We acknowledge the contribution of the Université Laval electronics staff, B. Boule, J. Laferrière, and R. Drolet, and the machinists, A. Bouffard and J. P. Langlois to the project. We also acknowledge the typing skills of J. Dagneault. We thank Dr. J. E. Hulse for the loan of the Pd(110) crystal.

Registry No. 3H-Diazirine, 157-22-2; palladium, 7440-05-3.

(52) Albert, M. R.; Yates, J. T., Jr. *The Surface Scientist's Guide to Organometallic Chemistry*; American Chemical Society: Washington, DC, 1987.